**Supplemental Table 1. Primers utilized to introduce sequence variations in Tg, AChE and secretory ChEL domain.** a. Amino acid positions are numbered in the precursor protein including the signal peptide of bTg or mouse Tg, reference sequences 7N4Y_1 and NP_033401.2 respectively. Bovine Tg substitution variants were generated in recombinant bTg expression plasmid (8). Equivalent amino acid positions to bTg C2444 and C2455 were manipulated in recombinant mouse ChEL (6) and in recombinant myc-tagged human AChE (9) to generate the indicated mutations. Mouse Tg variants at an amino acid equivalent to bTg K2225 were generated in recombinant mouse Tg expression plasmid (1) and in recombinant mouse ChEL expression vector (6). FP, forward primer; RP, reverse primer.

| Primer name | DNA sequence of the primers (5'—3') | Mutation |
|---|---|---|
| FP-Tg-C408A | CAGATTTACCGCATCCGCCCCACCCTCCATCAAG | **Bovine Tg-C408A** |
| RP-Tg-C408A | CTTGATGGAGGGTGGGGCGGATGCGGTAAATCTG | |
| FP-Tg-C608A | CAGCTCTCAGGGCGCCGGGCAGGCACCT | **Bovine Tg-C608A** |
| RP-Tg-C608A | AGGTGCCTGCCCGGCGCCCTGAGAGCTG | |
| FP-ChEL-C2444A | CCTTGGCAAAGGAGGTTGGAGCCCCTACTTCATCCATC | **Mouse ChEL-C2444A** |
| RP-ChEL-C2444A | GATGGATGAAGTAGGGGCTCCAACCTCCTTTGCCAAGG | |
| FP-ChEL-C2455S | CAGGAAGTGGTATCAAGTCTCCGCCAGAAGC | **Mouse ChEL-C2455S** |
| RP-ChEL-C2455S | GCTTCTGGCGGAGACTTGATACCACTTCCTG | |
| FP-Tg-K2225E | TGGGCACTGCCTGGGAGCAAGTATACCGG | **Mouse ChEL-K2225E and mouse Tg-K2225E** |
| RP-Tg-K2225E | CCGGTATACTTGCTCCCAGGCAGTGCCCA | |
| FP-AChE-C2444A | CCACCTTGTGGGCGCTCCTCCAGGCGGC | **Human AChE-C2444A-Myc** |
| RP-AChE-C2444A | GCCGCCTGGAGGAGCGCCCACAAGGTGG | |
| FP-AChE-C2455S | CAGAGCTGGTAGCCTCCCTTCGGACACG | **Human AChE-C2455S-Myc** |
| RP-AChE-C2455S | CGTGTCCGAAGGGAGGCTACCAGCTCTG | |
| FP-Tg-C2444A | CAAAGGAGGTTGGCGCCCCCAGCTCGTCTG | **Bovine Tg-C2444A** |
| RP-Tg-C2444A | CAGACGAGCTGGGGGCGCCAACCTCCTTTG | |
| FP-Tg-C2455S | CAAGAAATGGTGTCCTCCCTCCGCCAGGAG | **Bovine Tg-C2455S** |
| RP-Tg-C2455S | CTCCTGGCGGAGGGAGGACACCATTTCTTG | |

**Supplemental Table 2: Species-specific amino acid numbering of Tg, and secretory ChEL.** Residues equivalent to those in bovine Tg were identified using MegAlign (DNASTAR) to align the corresponding primary protein sequences. For simplicity, throughout the main text and the remaining portion of the supplemental text, all residues are referred to using numbering of bovine Tg, including signal peptide (UniProtA0A4W2CHS8). N/A: Not Applicable.
*Note: recombinant human Tg was not used in this study.

| Protein : | bovine Tg | mouse Tg | human Tg* | mouse ChEL domain |
|---|---|---|---|---|
| Amino acid numbering: species-equivalent positions | C408 | C408 | C408 | N/A |
| | C608 | C608 | C608 | N/A |
| | K2225 | K2222 | K2223 | K68 |
| | C2444 | C2441 | C2442 | C287 |
| | C2455 | C2452 | C2453 | C298 |

## Supplemental Figure Legends

**Supplemental Figure S1. Primary structure of Tg.**
Tg regions I, II, III and ChEL are indicated at the bottom of the representation. Tg domains are described above the regions, with amino acid numbering above derived from hTg.

**Supplemental Figure S2. WT and mutant Tg protein export from transfected thyrocytes.**
**A.** PCCL3 *TG* knockout (*TG*-KO) cells were either untransfected or stably transfected to express the indicated bTg constructs. Serum-free media (M) was collected for 48 h, the cells (C) were lysed, and both were analyzed by reducing SDS-PAGE, electrotransfer to nitrocellulose, and immunoblotting with polyclonal anti-Tg.
**B.** From 3 independent experiments like that shown in panel A, the relative secretion of Tg was calculated for each construct; mean ± S.D; *, $p < 0.05$.

**Supplemental Figure S3. Sites of contact between ChEL and Tg region I.**
Local structural representation of bovine Tg [PDB 7n4y (5)] prepared using UCSF ChimeraX (4). The contact interfaces between ChEL (in gold) and Tg region I from the same Tg monomer (in green). K2225 within ChEL is located at the contact interface #1. C2444 and C2455 (in pink) are at a distance from the contact interfaces.

**Supplemental Figure S4. Physical proximity between Tg-K2225 and Tg-W1090.**
**A.** Local structural representation from bovine Tg [PDB 7n4y (5)] was prepared using UCSF ChimeraX (4). The distance (in Å) between the closest atoms of K2225 (ChEL, in gold) and W1090 (region I, in green) is shown.
**B.** Structure from human Tg [PDB 6SCJ (2)].
**C.** Bioinformatic analyses of K2225 in ChEL (gold) and bTg region I (green) using Coot (3) and UCSF ChimeraX (4).

**Supplemental Figure S5. Absence of detectable disulfide bond between bTg-C2444 and bTg-C2455 by cryoEM.**
Electron density map and structural model with local resolution scale shown, highlighting C2444 and C2455, in which the two Cys side chains are pointing in opposite directions. Based on primary data in (5).

**Supplemental Figure S6. Role of the C2444-C2455 disulfide bond in the trafficking of AChE.**
**A.** Schematic of WT AChE from (7) highlights three intramolecular disulfide bonds with one disulfide loop (circled in red) that is equivalent to bTg C2444-C2455.
**B.** 293T were either nontransfected (NT) or transfected to express the indicated AChE-Myc constructs. After a 13 h period, the media (M) were collected and cells were lysed (C) and analyzed by SDS-PAGE under nonreducing (*left*) and reducing (*right*) conditions, electrotransfer to nitrocellulose, and immunoblotting with anti-Myc antibody. β-actin is a loading control.
**C.** From 3 independent experiments like that shown in panel B, the relative secretion of AChE-Myc was calculated for each construct; mean ± S.D; *, $p < 0.05$.

## References Cited in Supplement


1. Citterio CE, Morishita Y, Dakka N, Veluswamy B, Arvan P (2018) Relationship between the dimerization of thyroglobulin and its ability to form triiodothyronine. J Biol Chem 293:4860-4869.
2. Coscia F, Taler-Vercic A, Chang VT, Sinn L, O'Reilly FJ, Izore T, Renko M, Berger I, Rappsilber J, Turk D, Lowe J (2020) The structure of human thyroglobulin. Nature 578(7796):627-630.
3. Emsley P, Cowtan K (2004) Coot: model-building tools for molecular graphics. Acta Crystallogr D Biol Crystallogr 60:2126-2132.
4. Goddard TD, Huang CC, Meng EC, Pettersen EF, Couch GS, Morris JH, Ferrin TE (2018) UCSF ChimeraX: Meeting modern challenges in visualization and analysis. Protein Sci 27:14-25.
5. Kim K, Kopylov M, Bobe D, Kelley K, Eng ET, Arvan P, Clarke OB (2021) The structure of natively iodinated bovine thyroglobulin. Acta Crystallogr D Struct Biol 77:1451-1459.
6. Lee J, Di Jeso B, Arvan P (2008) The cholinesterase-like domain of thyrogobulin functions as an intramolecular chaperone. J Clin Invest 118:2950-2958.
7. MacPhee-Quigley K, Vedvick TS, Taylor P, Taylor SS (1986) Profile of the disulfide bonds in acetylcholinesterase. J Biol Chem 261:13565-13570.
8. Park YN, Arvan P (2004) The acetylcholinesterase-homology region is essential for normal conformational maturation and secretion of thyroglobulin. J Biol Chem 279:17085-17089.
9. Wang X, Lee J, Di Jeso B, Treglia AS, Comoletti D, Dubi N, Taylor P, Arvan P (2010) Cis and trans actions of the cholinesterase-like domain within the thyroglobulin dimer. J Biol Chem 285:17564-17573.

## Primary Structure of Thyroglobulin

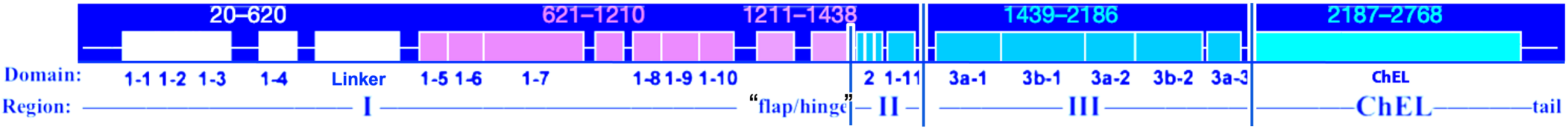


Citterio et al., Supplemental Figure S1

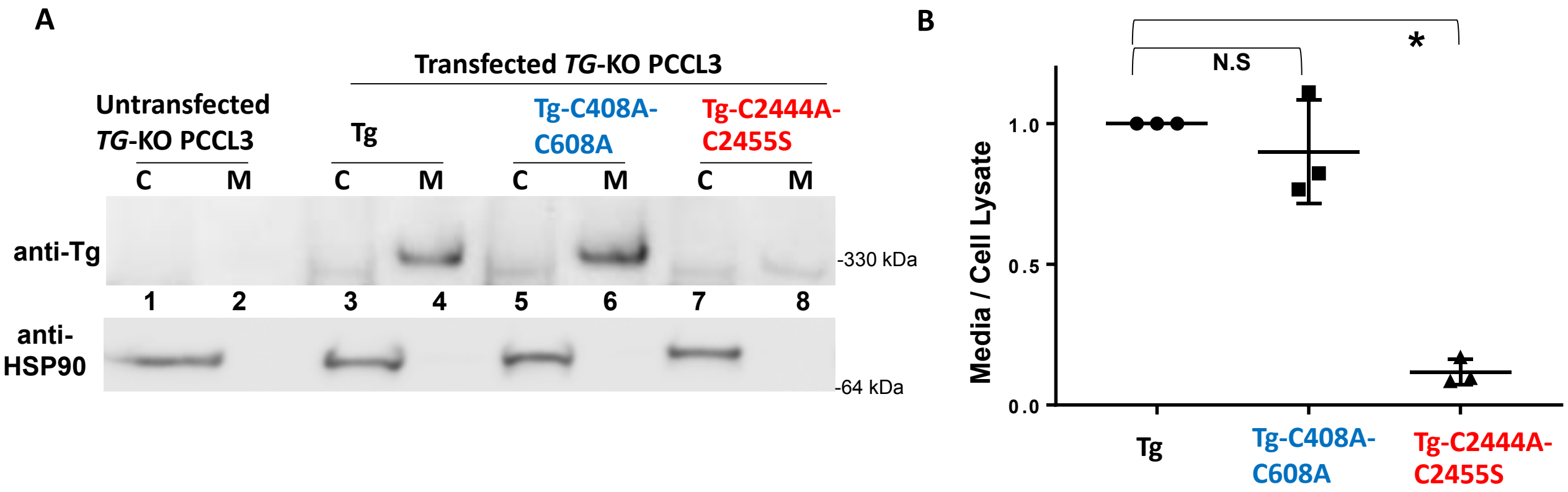


Citterio et al., Supplemental Figure S2

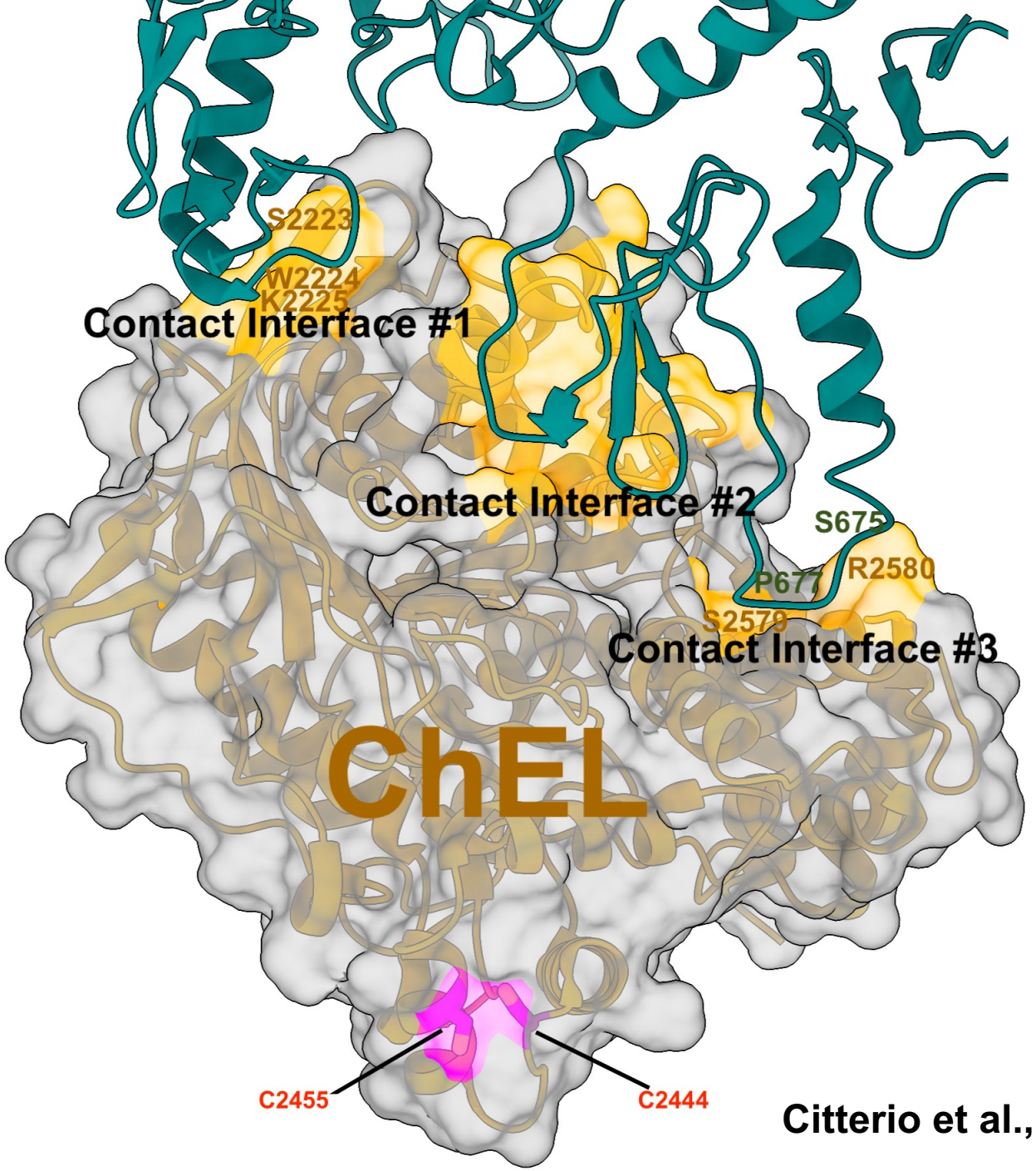


Citterio et al., Supplemental Figure S3

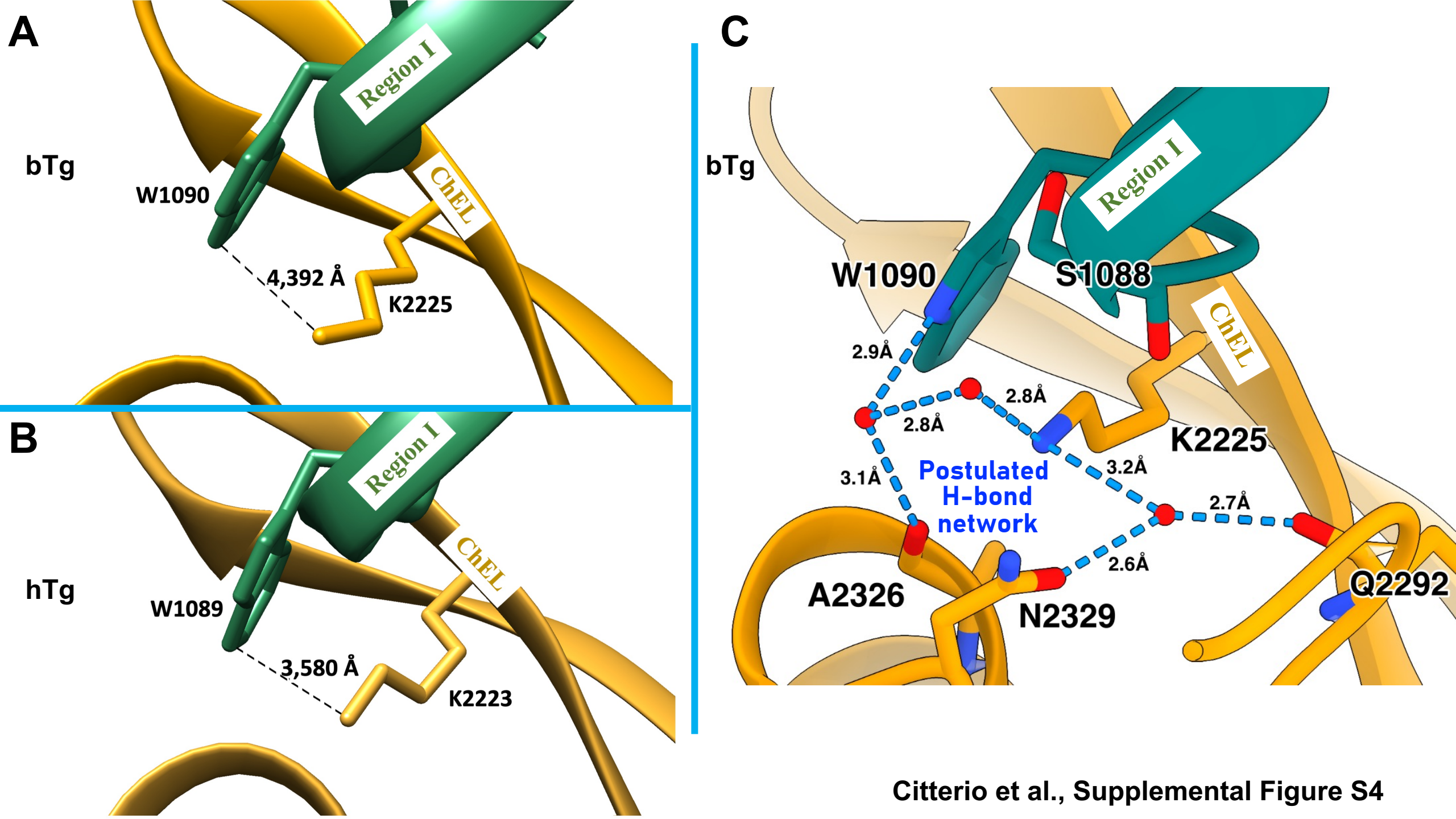


Citterio et al., Supplemental Figure S4

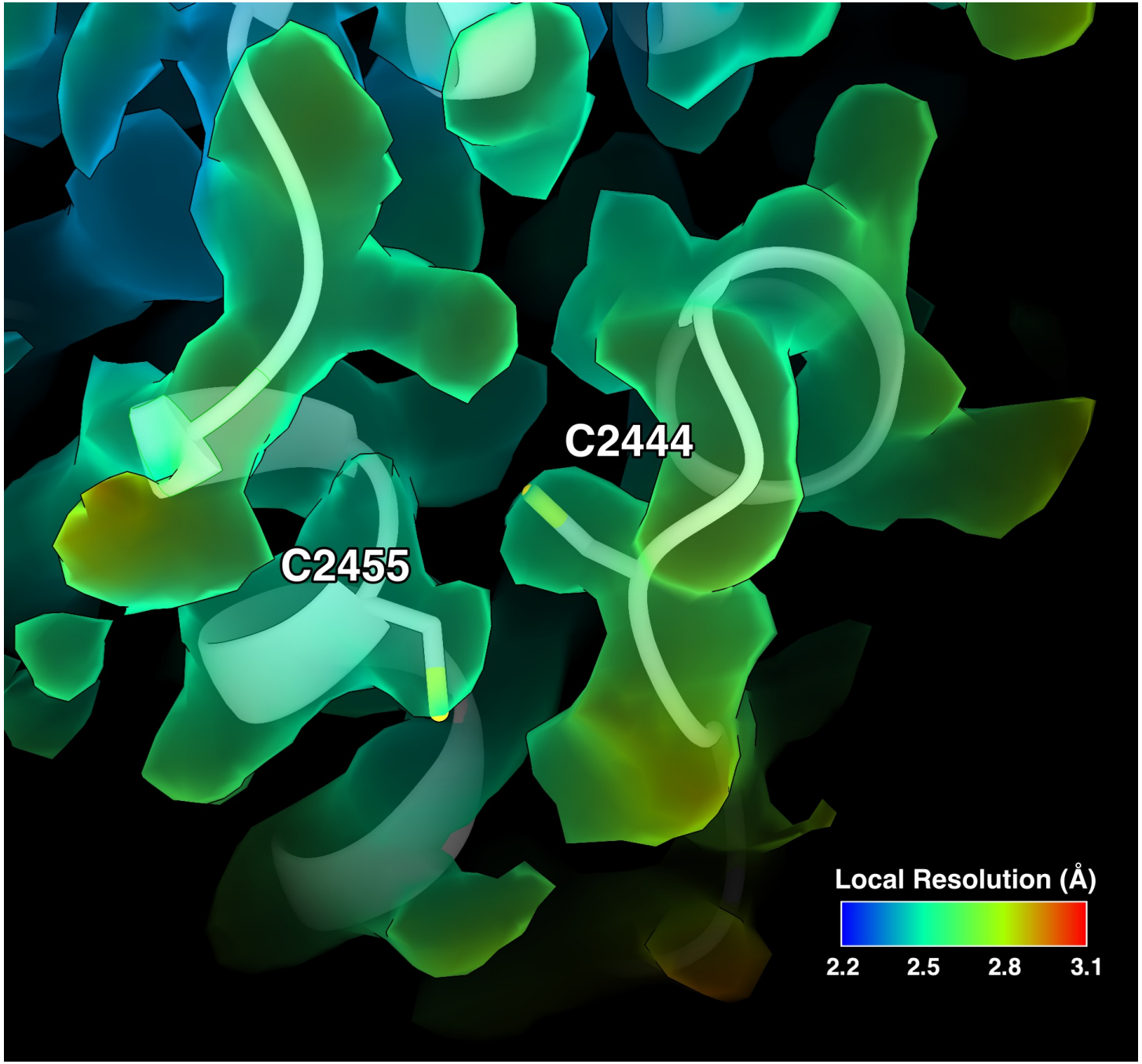


**Citterio et al.,**
**Supplemental Figure S5**

A

## Acetylcholinesterase

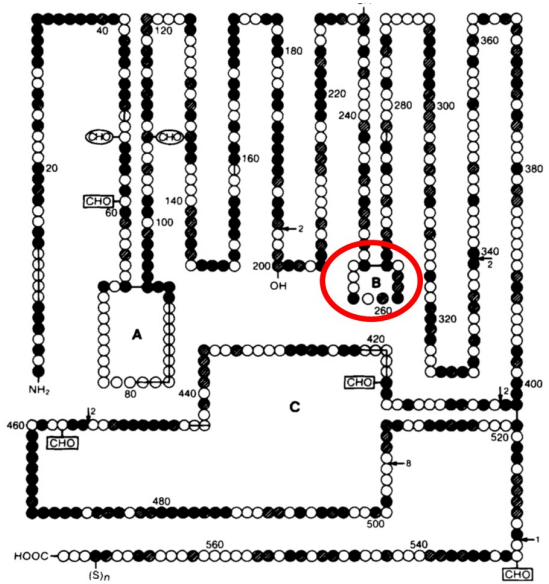

*J Biol Chem. 1986 Oct 15;261(29):13565-70.*

B

## Nonreducing

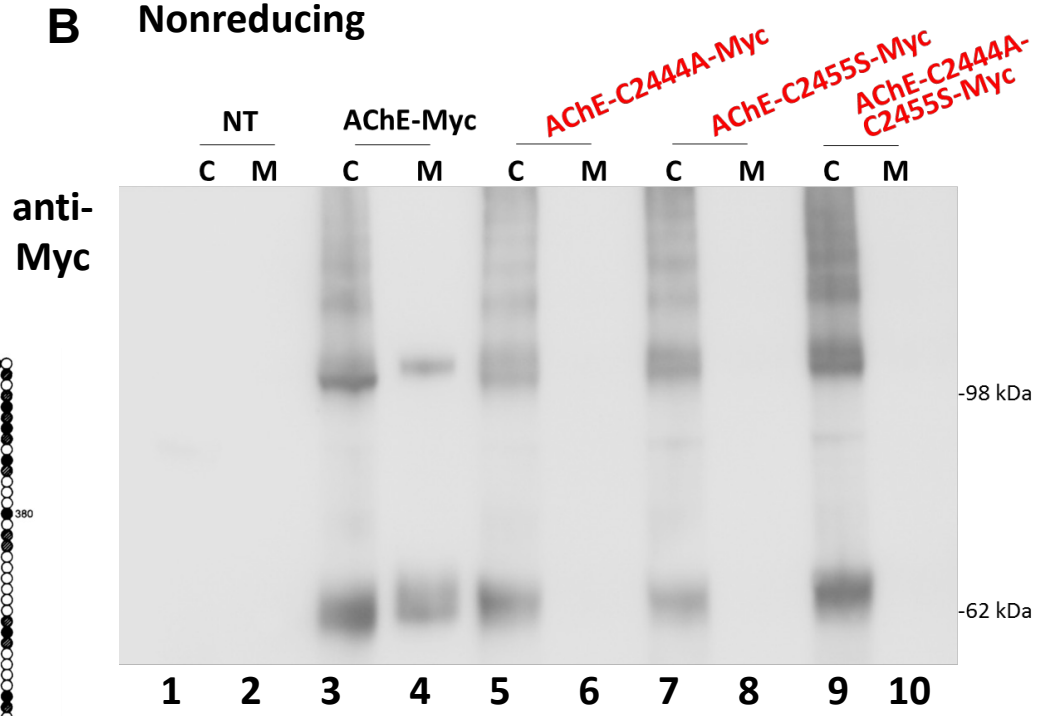


## Reducing

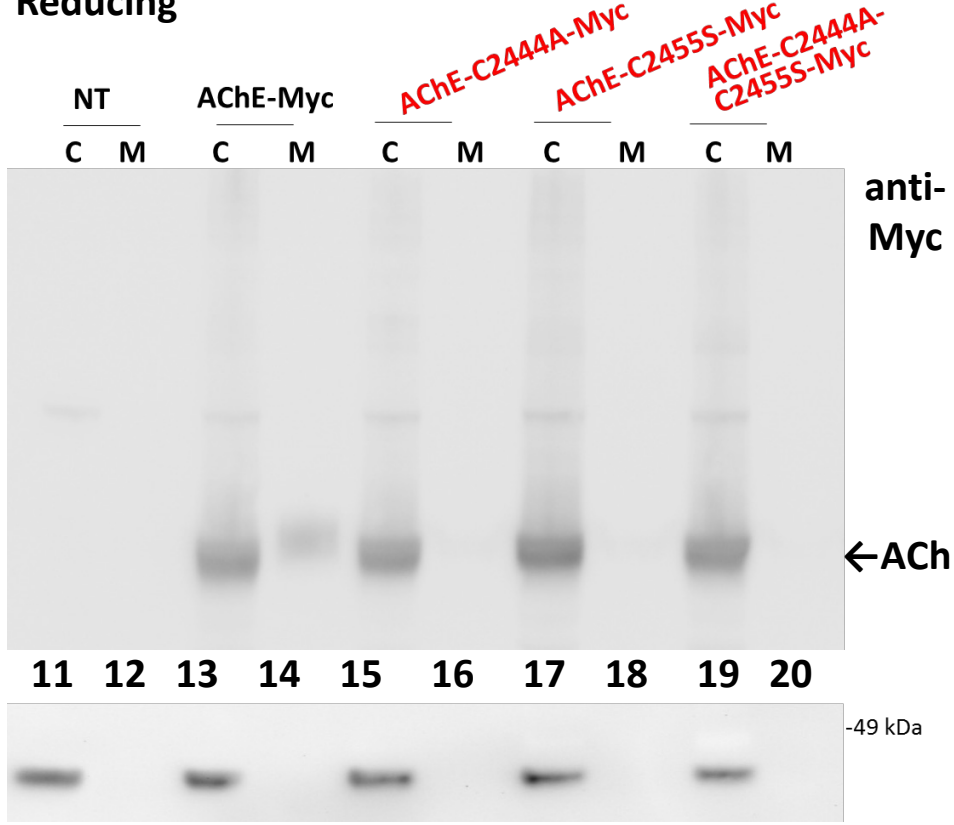


C

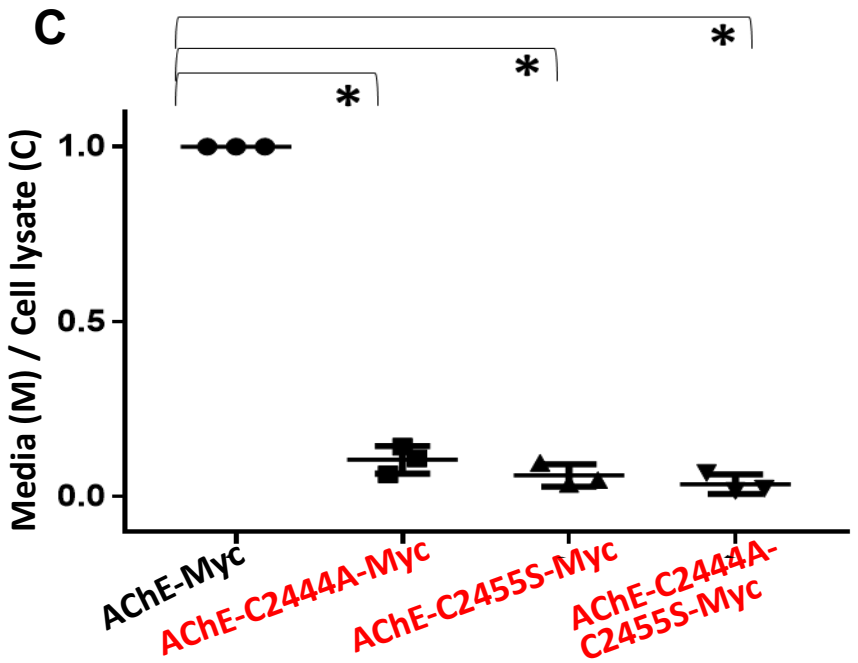


**Citterio et al., Supplemental Fig. S6**